Zeitschrift: IABSE proceedings = Mémoires AIPC = IVBH Abhandlungen
Band: 10 (1986)
Heft: P-104: Fatigue strength of tension flanges with stud shear connectors

Artikel: Fatigue strength of tension flanges with stud shear connectors
Autor: Maeda, Yukio / Kajikawa, Yasuharu
DOI: https://doi.org/10.5169/seals-39613

Fatigue Strength of Tension Flanges with Stud Shear Connectors

Résistance à la fatigue des semelles tendues avec goujons

Ermüdungsfestigkeit von Zuggurten mit Kopfbolzendübeln

Yukio MAEDA
Prof. of Civil Engineering
Kinki University
Osaka, Japan

Yukio Maeda was formerly a Professor of Civil Engineering at Osaka Univ., where he was awarded the title of Professor Emeritus in 1985. He has been a Professor at Kinki Univ. since April 1985. He is Vice-Chairman of the Technical Committee of IABSE.

Yasuharu KAJIKAWA
Head of Dev. Section
KAWADA Construction Co., Ltd.
Osaka, Japan

Yasuharu Kajikawa, born 1944, was formerly an Assistant Professor of Civil Engineering at Osaka Univ., where he obtained the degree of Dr. Eng. in 1985. Since April 1985 he has been engaged in research on the construction of steel and concrete bridges at KAWADA Construction Co.

SUMMARY

The fatigue tests which were conducted by the authors on beam-type and coupon-type specimens showed that the fatigue strength of flange plates with stud shear connectors decreases in proportion to increasing shear forces acting on the studs. The effects of the shear forces were examined using a three-dimensional finite element stress analysis at the stud base and evaluated reasonably by an effective stress at the toe of the weld. Finally, a method for the fatigue design of the plate was proposed.

RÉSUMÉ

Les essais de fatigue qui ont été menés par les auteurs sur des échantillons, du type poutre et du type éprouvette de traction, ont montré que la résistance à la fatigue des semelles avec goujons diminuait avec l'augmentation des efforts de cisaillement agissant sur les goujons. Les effets des efforts de cisaillement ont été examinés au moyen d'une analyse de contraintes par éléments finis tridimensionnels à la base du goujon et évalués en utilisant une contrainte effective au pied de la soudure. Finalement, une méthode pour définir la résistance à la fatigue de la semelle a été proposée.

ZUSAMMENFASSUNG

Die von den Autoren auf Versuchsträgern und Zugproben durchgeführten Ermüdungsversuche haben gezeigt, dass die Ermüdungsfestigkeit von Gurtplatten mit Schubdübeln im Verhältnis zur Zunahme der auf die Dübel wirkenden Scherkräfte abnimmt. Der Einfluss der Scherkräfte wurde anhand einer Spannungsanalyse mit dreidimensionalen finiten Elementen an der Dübelbasis untersucht und durch die Einführung einer effektiven Spannung am Fusse der Schweissnaht erfasst. Schliesslich wird eine Methode zur Bestimmung der Ermüdungsfestigkeit von Zuggurten vorgeschlagen.

1. INTRODUCTION

In a steel-concrete composite beam under repeated negative bending moment, as observed in negative moment regions of continuous composite girders for highway bridges, the steel flange plate on which stud shear connectors have been welded is subjected to combined stresses of flexural tensile stress in the plate and shearing stress on the connectors. The fatigue strength of the flange has been obtained by several experiments. Selby et al. [1] in U.S.A., Roshardt [2] in West Germany and Wakabayashi et al. [3] in Japan tested 'coupon-type' specimens under uniaxial extension, which consisted of a flat plate and of one or more studs welded to it. Kunihiro et al. [4] in Japan, Welz et al. [5] in West Germany and Selby et al. [1] reported that the bending fatigue strength of a bare flange plate of a H-shaped beam on which studs were welded, was nearly equal to the coupon-type test results. Furthermore, Kunihiro et al. [6] pointed out that the shearing force on the studs would affect the fatigue strength of the flanges, from the test results on composite beam model specimens ('beam-type' specimens) subjected to repeated negative moment, but they failed to obtain quantitative results. It has been known especially in composite beams that difficulty in estimating the actual fatigue strength of the flange plate would be primarily caused by a complex 'combined stress condition', which would occur due to both tension of a plate and shear of a stud at the root of the stud.

In this paper, the effects of shearing forces upon the fatigue strength of a flange are examined by two different fatigue tests of beam-type and coupon-type specimens. Fatigue characteristics of the flange plate under combined loading are interpreted by means of the three-dimensional finite element stress analysis. An estimating method for the fatigue strength of the flange plate is presented, and then a fatigue design method of the plate is proposed.

2. FATIGUE TEST OF BEAM-TYPE SPECIMENS [7]

2.1 Outline of Test

All of the beams have the same cross-section, but the loading condition for E-series is different from H-series as shown in Fig. 1. In each specimen, combinations of longitudinal reinforcements (in terms of the diameter, D) embedded in the slab and stud spacings along the beam were decided as shown in Table 1. As the result of the material test, the yielding point, the tensile strength and the elongation for the steel beam of which grade was SS41 by JIS (Japanese Industrial Standards) designation, were 279 MPa, 444 MPa and 30 %, respectively. The mean compressive strength of the slab concrete was 30 MPa.

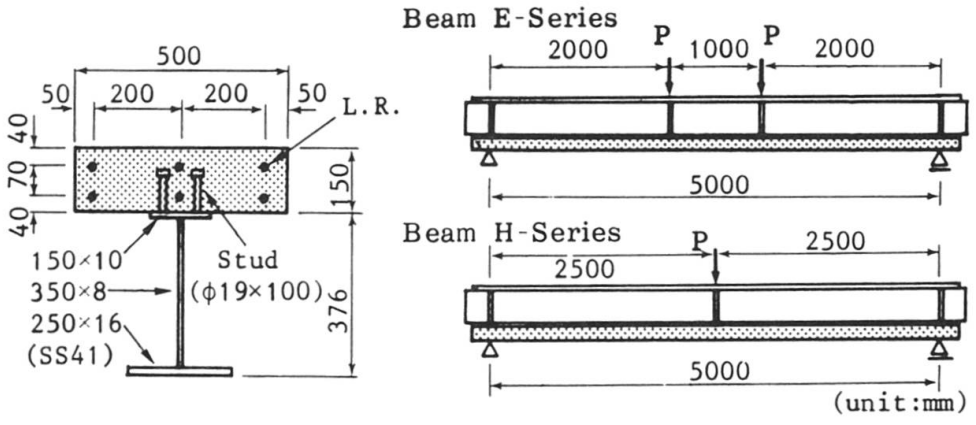

Fig. 1 Cross-section and loading points of beam specimens.

The beam was simply supported with the span length of 5 meters, setting the concrete slab upside down as shown in Fig. 1. Repeated negative bending moments were applied to the steel flange of the beam by using hydraulic jacks of a Losenhausen-type fatigue testing machine at the rate of about 5 Hz.

2.2 Test Results

The results of the fatigue tests are summarized in Table 1. σ_{tr} and τ_r are the stress ranges acting at the location of failure points (see the illustration in the table) during the fatigue tests. They were calculated by applying the incomplete interaction theory taking account of relative slips at the interface between steel and concrete, and by assuming that a cross-section consisting of both the longitudinal reinforcements embedded in the slab and the steel beam acts effectively against the negative moment.

In all of the fractured beams, a fatigue crack which was initiated at the toe of a welded stud propagated across the tension flange with repetition of the loading and finally penetrated into the web plate as shown in Fig. 2, which indicated a part of the steel beam near the loading point. Illustrations in Table 1 show that all the

Table 1 Summary of beam specimens and fatigue test results.

Beam No.	D (mm)	p (cm)	σ_{tr} (MPa)	τ_r (MPa)	N_f ($\times 10^4$ cycles)	Location of Failure in Tension Flange (cm)
E1-1	D13	40	103	14	200 →	
E1-2			103	14	300 →	
E2-1-1	D16	30	123	38	125	
E2-1-2			105	32	222.6	
E2-2-1	D16	60	83	52	75	
E2-2-2			70	44	196	
E2-3-1	D16	10	93	7	200 →	
E2-3-2			135	1	133	
E3-1	D19	20	116	23	145.8	
E3-2			81	28	222.7 →	
H1-1	D16	30	80	25	280	
H1-2			122	22	90	
H1-3			156	28	60	

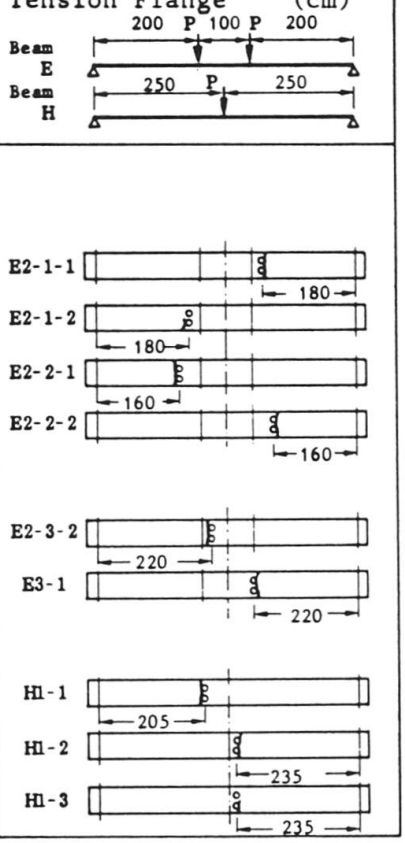

D : Diameter of Longitudinal Reinforcement in Slab
p : Stud Spacing
σ_{tr}: Stress Range in Tension Flange
τ_r : Shear Stress Range on a Stud
N_f : No. of Cycles to Failure of Tension Flange
→ : No Failure

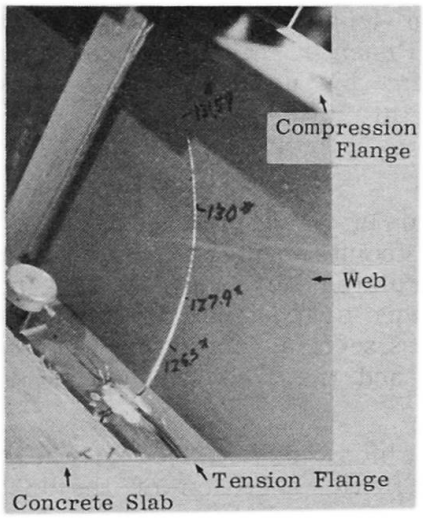

Fig. 2 Fatigue crack propagation.

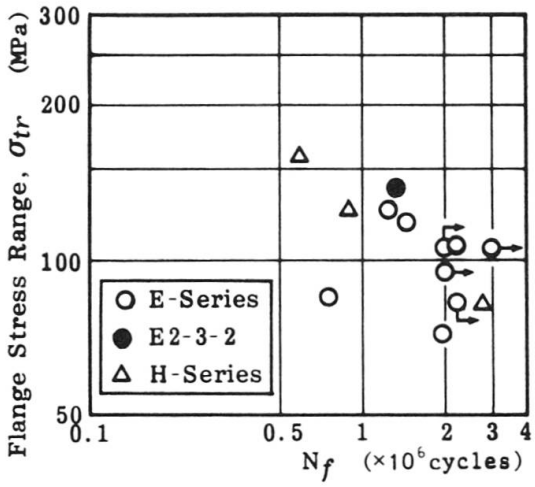

Fig. 3 S-N relations for beam specimens.

fatigue cracks except for only E2-3-2 are located in the 'shear span' where the vertical shear force coexists with the bending moment.
Fig. 3 shows S-N relationships expressed in terms of flexural stress ranges in the tension flange, σ_{tr}. The points vary widely and the fatigue strength at two million cycles is only about 80 MPa. These would have been caused by changes in material properties due to the welding heat, occurrence of weld residual stress, stress concentration due to the discontinuity of geometrical shape at the root of the stud, and so on. Judging from the above-mentioned conditions for the crack initiation, however, it can be known that the horizontal shear force which acted on the stud shear connector must be a more important influence factor for the fatigue life of the tension flange.

3. FATIGUE TEST OF COUPON-TYPE SPECIMENS [8]

In the beam tests, a S-N relationship for any constant shear stress level could not be obtained, because it was difficult to vary arbitrarily the combination of the flexural tensile stress in the tension flange with the shear stress on the stud, and besides, to evaluate exactly the horizontal shear force in the beam specimens. Then, fatigue tests were conducted with coupon-type specimens consisting of a flat steel plate and a headed stud which was welded on it.

Table 2 Material properties of coupon specimens.

Material	Chemical Composition (wt %)						Mechanical Properties		
	C	Si	Mn	P	S	Cu	σ_y MPa	σ_t MPa	ϵ %
Plate(SS41)	0.17	0.04	0.77	0.009	0.031	—	275	451	31
Plate(SM50A)	0.14	0.45	1.32	0.018	0.014	—	353	530	31
Plate(SM58Q)	0.14	0.36	1.21	0.019	0.012	0.03	549	628	20
Stud (ϕ19)	0.17	0.01	0.69	0.011	0.033	—	275	422	30

3.1 Outline of Test

Three kinds of structural steels, JIS SS41, SM50A and SM58Q, were used for the test specimens. The headed studs were made of the steel which conformed JIS B 1198-1982 'Headed Studs.' Those material properties are given in Table 2. Shapes and dimensions of the specimens are shown in Fig. 4.

Four test series, A, B, C, and D, were prepared in order to examine systematically the effect of stud welding upon the tensile fatigue strength of the plate. A-series is to obtain a basic S-N curve for plain plate of the base material. B-series is to estimate the effect of welding on the base material by using specimens in which the stud was completely removed by grinding the weld upset, which is also called a weld collar or a flush, around the root of the stud for excluding the effect of the geometrical discontinuity. C-series is to determine a S-N curve under the condition that a stud is not subjected to any shear force, namely in the state of a bare stud as welded. Almost all of the fatigue strengths of the 'steel plate with studs' have been obtained by using this type of specimens.
For reproduction of the stress condition similar to observation in actual composite beams, the authors developed a unique fatigue testing method by using coupon-type specimens, which consisted of a flat steel plate and a welded stud encased in a concrete block, namely D-series as shown in Fig. 4. Fig. 5 shows schematically a new loading apparatus [8] in which the pulsating shear force can act on the stud in the same phase as the pulsating tension of the plate.

A Losenhausen-type fatigue testing machine was used for all the test series. The pulsating tension with the minimum load of 10 kN and the rate of 6 ∿ 8 Hz was applied to the plate for A-, B- and C-series. In D-series, the plates were subjected to similar tension to the other series at three different levels of the shear stress range, τ_r, approximately 20, 40 and 60 MPa, which was selected as a parameter for the S-N relation of each steel and calculated for a nominal cross-section of the stud shank.

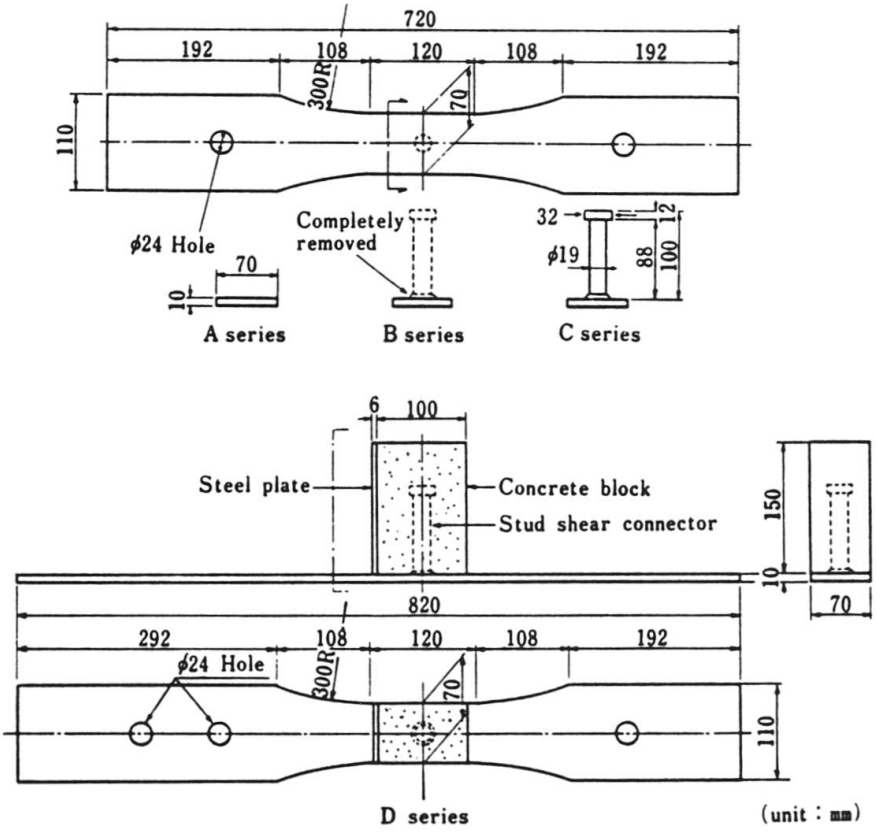

Fig. 4 Coupon specimens.

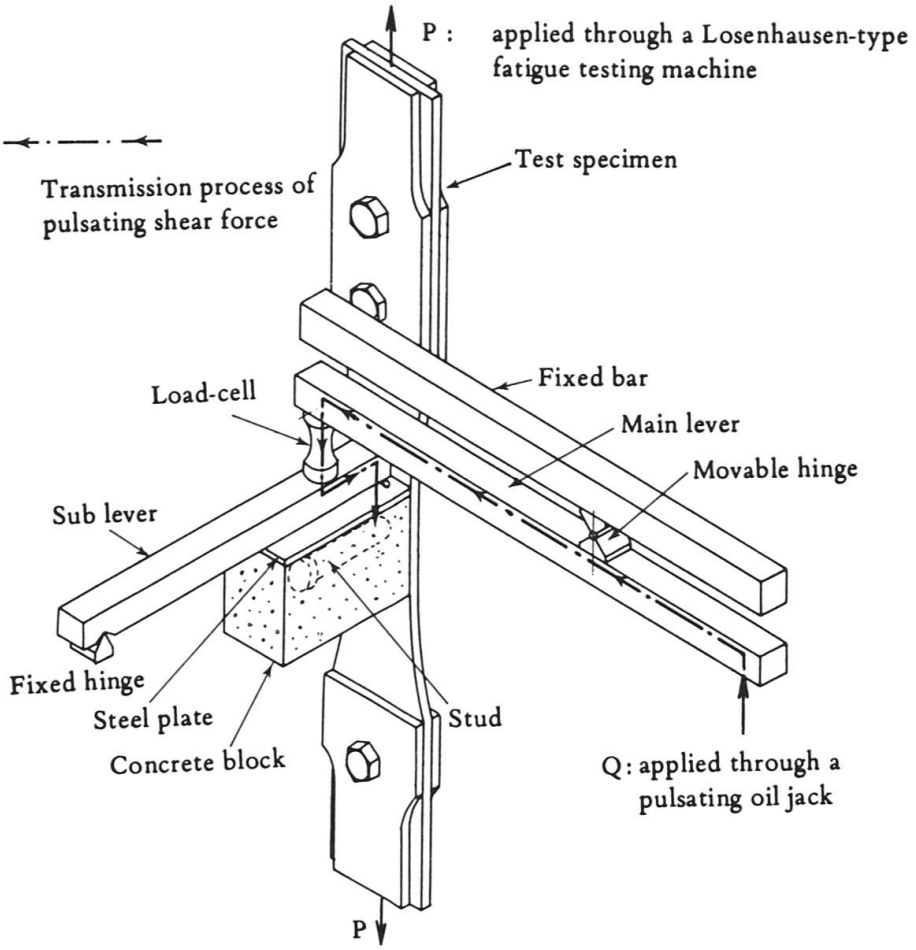

Fig. 5 Schematic diagram of combined loading.

3.2 Test Results

The results of the fatigue tests for each steel are presented in the form of S-N diagrams in Figs. 6 ∿ 8, on the basis of log-log relationship between the nominal applied tensile stress range in the plates, σ_r, and the number of cycles to failure, N_f.

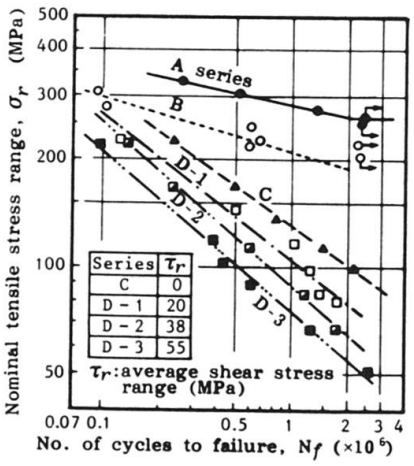

Fig. 6 S-N relations for SS41 steel.

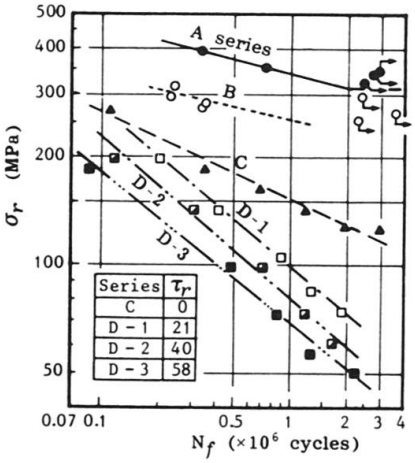

Fig. 7 S-N relations for SM50A steel.

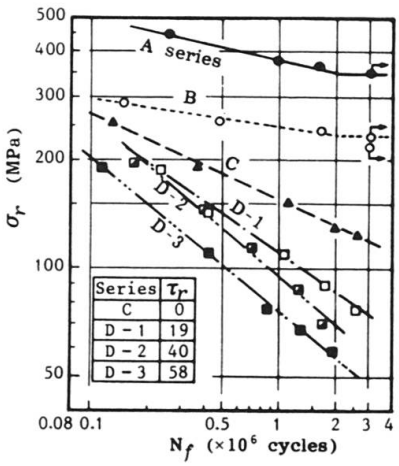

Fig. 8 S-N relations for SM58Q steel.

Since the S-N relationships for the test series (A ∿ D) show similar tendency for three kinds of steels (SS41, SM50A, SM58Q), the following discussions are mainly referred to the results for SS41 steel in Fig. 6.
The fatigue strength of B-series is lower about 70 MPa than that of A-series throughout the cycle lives. This reduction would have been primarily caused by the stress concentration due to internal weld defects such as blow-holes or lacks of fusion, because all of the fatigue cracks in B-series were initiated at the locations of these defects.
Besides, the fatigue strength of C-series reduced furthermore. In all of the specimens of C-series, a fatigue crack was initiated at either one of the upset edges closest to the ends of the plate, and propagated more rapidly toward the both sides of the plate, whereas no crack initiation was observed at internal weld defects as seen in B-series. Accordingly, it can be understood that the stress concentration due to the geometrical discontinuity at the toe of weld upset had a great influence on the fatigue strength of the plate.
All of the specimens of D-series also failed due to the propagation of a fatigue crack which had been initiated at the upset edge closest to the side of applied shear force. A typical fracture surface is shown in Fig. 9(b). As compared with Fig. 9(a) for C-series, it is seen that the fracture surface in D-series is not smooth and includes a narrow region where a crack has propagated along a fusion line due to the presence of shear force acting on the stud, while the fatigue crack in C-series has propagated approximately perpendicular to the plate surface and formed a relatively flat fracture surface.

By comparing four S-N curves of C, D-1, D-2 and D-3 series which are given in respective Figs. 6 ∿ 8, it is evidently noticed that the fatigue strength of the plate at any cycle life reduces gradually as the shear stress range, τ_r, increases. When the correlation between tensile stress ranges at two million cycles and shear stress ranges was investigated, it was found out that the fatigue strength of the plate decreased nearly in proportion to an increase of the shear stress, and that its relation had little difference for the three steels.

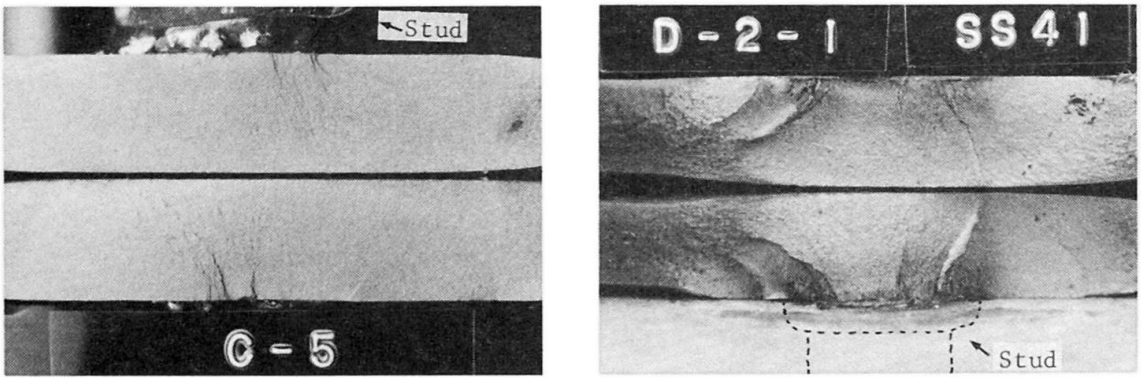

(a) C-series (b) D-series

Fig. 9 Typical fracture surface of coupon specimens.

4. STRESS ANALYSIS AT THE ROOT OF STUD

Though headed studs essentially function as shear connectors to transfer the shearing force at the interface between steel and concrete, its behavior has not been clarified yet because those used to be encased in concrete. From the above-mentioned test results, it is considered that the stress concentration due to geometrical discontinuity at the root of stud must be a more predominant factor

for the fatigue failure or the reduction of fatigue strength. Moreover, it can be supposed that this stress concentration will be accelerated by a shearing force on the stud. To clarify the stress condition at the root of stud, then, a three-dimensional stress analysis was carried out by using the Finite Element Method (FEM) for an elastic continuum.

4.1 Outline of Three-Dimensional FEM

The steel part of a test specimen of D-series, namely a steel plate and a headed stud, was replaced by a model consisting of a flat plate and columns. The measurement showed that the shape and size of the actual weld upset were rather irregular, and its diameter, height and contact angle were approximately $1.3d$, $0.25d$ and $40° < \theta < 140°$, respectively. Here, d is a diameter of stud shank and θ is an angle between the side of the upset and the surface of the plate. The half model was divided, for its symmetry, into a mesh as shown in Fig. 10 by using linear elements such as triangular prism, quadrangular prism and rectangular brick, of which degree of freedom for deformation was three per a node. For a simple consideration of relative slips or separations between steel and concrete, linkage elements which have only spring stiffeness and no volume, were used on the contact surface between steel and concrete to connect them. Though the angle θ had undoubtedly a large influence on the stress concentration, it was tentatively determined as 90° for laying emphasis on what stress condition occurs at the root rather than on what value is computed for the stress concentration factor, and besides for convenience of the element mesh division. Other models with different

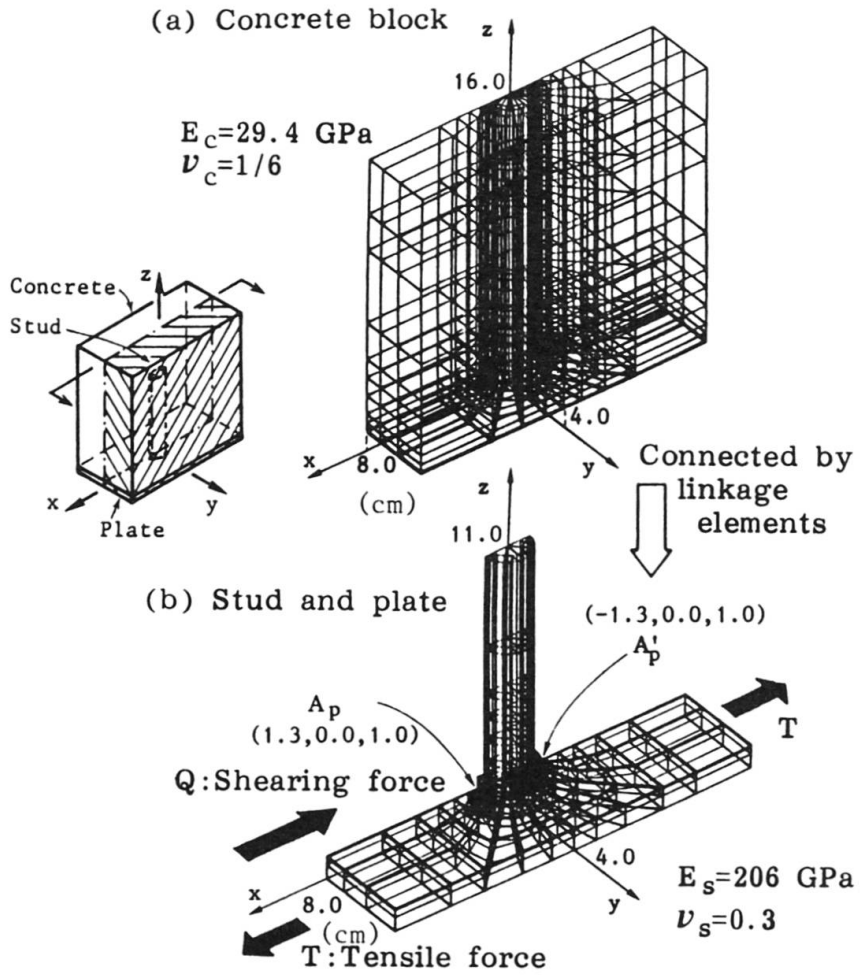

Fig. 10 Finite element mesh division.

shape and size of the upset could not be analyzed because of enormous computer time. In Fig. 10(b), the point Ap or Ap' is a location where the largest stress concentration will occur as described later, and also is an intersection point between the edge of upset and z-x plane.

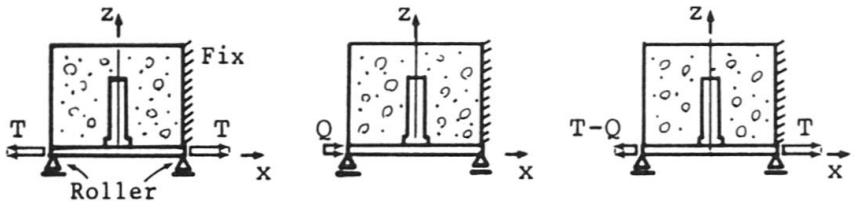

(a) Tension of Plate (b) Shearing of Stud (c) Combined tension and shear

Fig. 11 Loading and boundary conditions.

4.2 Stress Condition at the Root of Stud

4.2.1 Tension of Plate

The tensile force, T, was applied to the both sides of a plate under such a boundary condition as shown in Fig. 11(a), and its magnitude was 100 MPa as a mean stress which was uniformly distributed on the cross-section of the plate. The stresses in the plate on x, y and z directions of the co-ordinate through the point Ap were obtained. Fig. 12 shows a stress distribution of the stress component, σ_x , of which direction coincides with the tensile direction. It is evidently observed that the stresses concentrate three-dimensionally to form a peak at the point Ap or Ap'.

On the stress concentration in a plate with a stud under tension only, it was found out that the stress component in the loading direction, σ_x , was remarkable among six components. The point of the maximum stress, Ap or Ap' almost coincided with the location of crack initiation in the test specimens. Accordingly, it can be realized that the geometrical discontinuity at the toe of the weld upset must be the most predominant factor for the reduction of the fatigue strength under the tension.

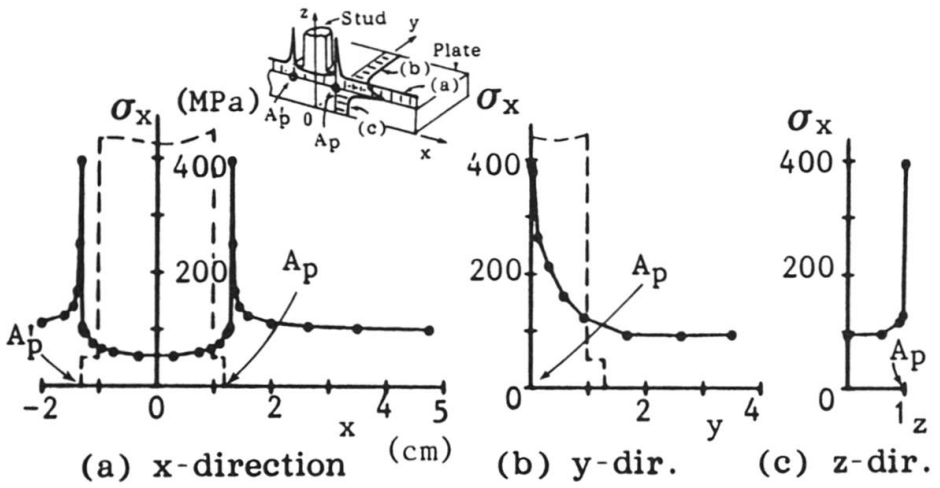

Fig. 12 Stress distributions under tension only.

4.2.2 Shearing of Stud

The shear force, Q, was loaded on the stud by fixing one side of a concrete block and by applying an uniformly distributed compressive force which was equivalent to a shear force of 10 kN to the opposite side of a steel plate (see Fig. 11(b)). The stress condition in the vicinity of the point Ap in the plate was similar to that for the tension only, and the stress component in the loading direction, σ_x , too, formed the largest stress concentration. Fig. 13 shows a stress distribution of σ_x . In Fig. 13(a), σ_x distributes along x-axis antisymmetrically about the center of the stud shank, namely, the tensile stress occurs at the loading side of the shear force (point Ap side) and the compressive stress occurs at the opposite side (point Ap' side). The maximum value of the tensile stress at the point Ap is nearly equal to that for the tension only. It can be considered that such a large stress concentration occurs because of the state of 'overlapped stress concentration', which is caused by a sudden change of applied force in the plate (i.e. dynamical discontinuity) in addition to the geometrical discontinuity.

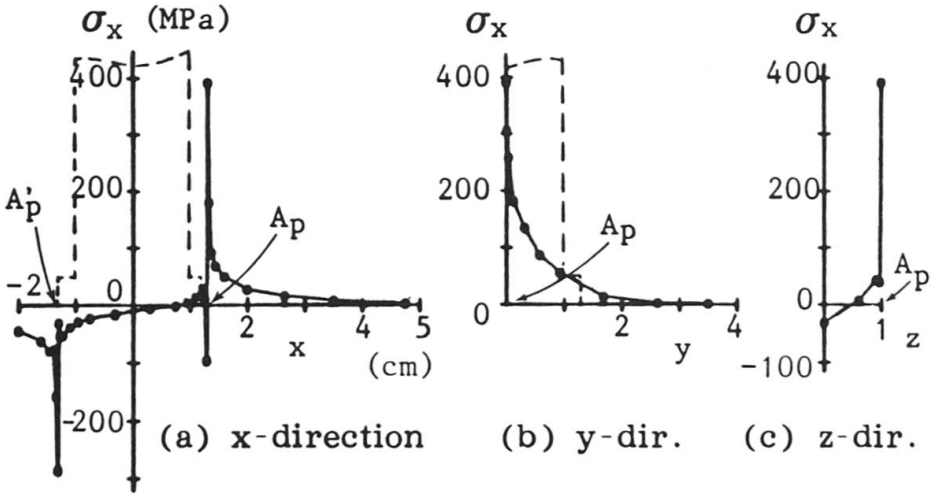

Fig. 13 Stress distributions under shear only.

4.2.3 Combined Tension and Shear

The combined tension and shear loads were applied as shown in Fig. 11(c). Two different tensile forces T-Q and T were given at the both ends of the plate, and the difference between them, Q, acted on the stud as a shear force which was resisted by the stud through a concrete block. The mean tensile stress was 100 MPa and the shear force was 10 kN.

The deformations of a symmetrical section (z-x plane at y=0) and the displacements of nodes at the contact surface between steel plate and concrete block are shown in Fig. 14. In the vicinity of the stud upset as seen in Fig. 14(a), it is seen that the concrete part on the loading side of shear force is locally compressed by the stud without caving into the steel part, that the separation between steel and concrete arises on the opposite side of shear force, and that the steel plate at the base of the stud is deformed wavelikely. Also in Fig. 14(b), the relative slips between steel and concrete are given.

The stress distributions of σ_x are shown in Fig. 15 in the same form as Fig. 12. σ_x distributes along x-axis unsymmetrically about the center axis of the stud shank with a extremely large stress concentration at the point Ap, namely at the toe of the upset on the loading side of the shear force. The shape and magnitude of the stress distribution are nearly equal to those obtained by superposing the case of tension (Fig. 12) and that of shear (Fig. 13).

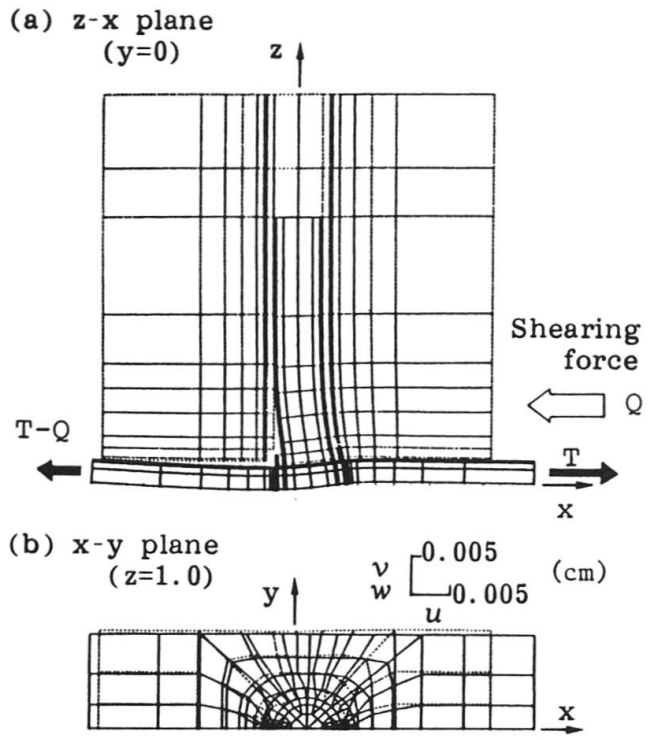

Fig. 14 Displacements of node under combined tension and shear.

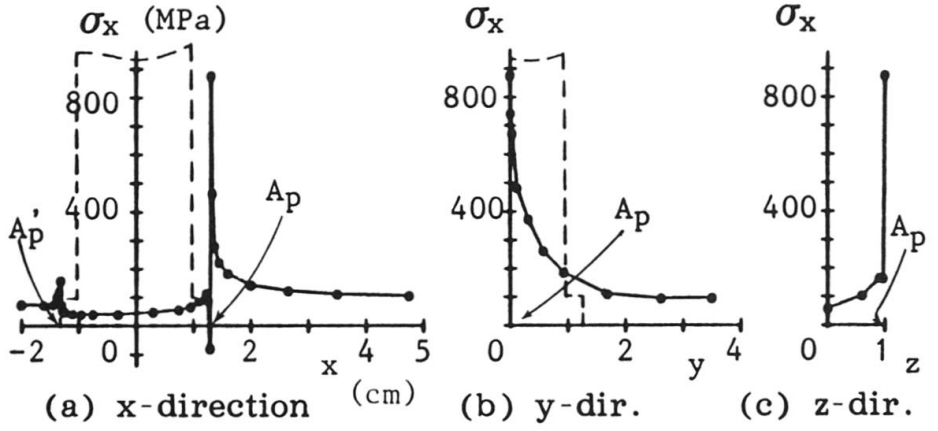

Fig. 15 Stress distributions under combined tension and shear.

Fig. 16 shows a maximum principal stress distribution in the vicinity of the point Ap in a symmetrical section (z-x plane at y=0). The flow of tensile principal stresses in the plate is distorted at the corner point Ap due to the both of geometrical discontinuity and shear force, and a large amount of the stresses penetrate into the stud shank through the weld upset. The principal stresses, too, were distributed similarly to those obtained by superposing the case of tension and that of shear. The broken line in the figure shows the approximate propagating path of a fatigue crack which was observed in the test for D-series. Its direction is nearly perpendicular to the flow of the principal stresses throughout the length. From these facts, the fracture process under the combined loading could be explained to a certain extent.

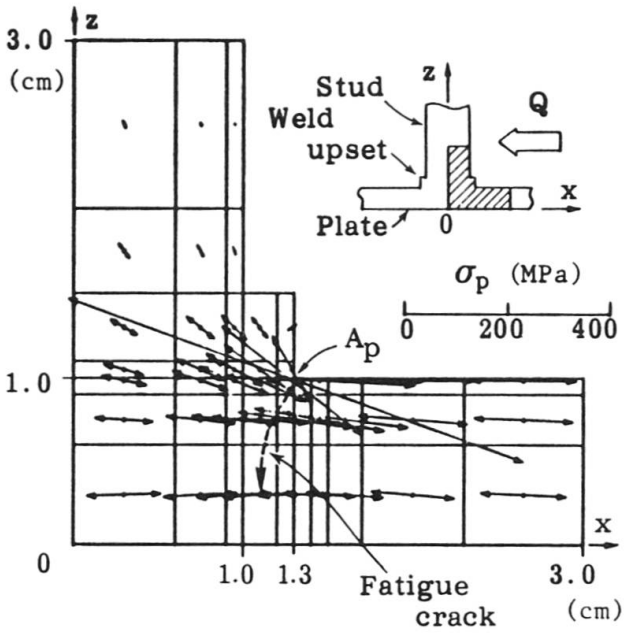

Fig. 16 Principal stress distributions at the base of stud under combined tension and shear.

5. ESTIMATION OF FATIGUE STRENGTH

If the coupon-type test results are applied to the estimation of the fatigue strength of the tension flange with welded studs in actual composite beams, the relationships between both the test results of beam-type and coupon-type specimens must be clarified in advance. An approach to consistent evaluation of the two different test results is presented.

5.1 Stress for Evaluation

As the results of the stress analysis, it was realized that the stress condition at the base of the stud was in a complex, three-dimensional combination, and that the normal stress component in the loading direction, σ_x , was remarkable under any loading condition, resulting in large stress concentration at the toe edge of the stud upset. Accordingly, it might be assumed that the fatigue strength could be evaluated by an 'effective stress', σ_e , which is sometimes called a 'generalized stress' or an 'equivalent stress.' It is calculated from six stress-components by the following equation;

$$\sigma_e=\frac{1}{\sqrt{2}}\left\{(\sigma_x-\sigma_y)^2+(\sigma_y-\sigma_z)^2+(\sigma_z-\sigma_x)^2+\frac{1}{6}(\tau_{yz}^2+\tau_{zx}^2+\tau_{xy}^2)\right\}^{\frac{1}{2}} \qquad (1)$$

where $\sigma_x, \sigma_y, \sigma_z$: normal stress components,
$\tau_{yz}, \tau_{zx}, \tau_{xy}$: shearing stress components.

Furthermore, it was found that all the stress components under the combined loading could be approximately calculated by the superposition of both tensile and shearing stress conditions. Then, the effective stress under the combined loading also could be computed by using nominal stresses and stress concentration factors for each case as follows:

$$\sigma_e=\sqrt{\alpha^2\cdot\sigma_0^2+\beta^2\cdot\tau_0^2+\gamma\cdot\sigma_0\cdot\tau_0} \qquad (2)$$

where

$$\alpha^2=\frac{1}{2}\left\{(\alpha_x-\alpha_y)^2+(\alpha_y-\alpha_z)^2+(\alpha_z-\alpha_x)^2+\frac{1}{6}(\alpha_{yz}^2+\alpha_{zx}^2+\alpha_{xy}^2)\right\},$$

$$\beta^2=\frac{1}{2}\left\{(\beta_x-\beta_y)^2+(\beta_y-\beta_z)^2+(\beta_z-\beta_x)^2+\frac{1}{6}(\beta_{yz}^2+\beta_{zx}^2+\beta_{xy}^2)\right\},$$

$$\gamma=(\alpha_x-\alpha_y)(\beta_x-\beta_y)+(\alpha_y-\alpha_z)(\beta_y-\beta_z)+(\alpha_z-\alpha_x)(\beta_z-\beta_x)+6(\alpha_{yz}\cdot\beta_{yz}+\alpha_{zx}\cdot\beta_{zx}+\alpha_{xy}\cdot\beta_{xy}).$$

and σ_0 : the nominal stress under tension only, namely, the nominal mean tensile stress on a cross-section of a plate,

$\alpha_x, \alpha_y, \cdots, \alpha_{xy}$: the stress concentration factors for each stress component under tension only,

τ_0 : the nominal stress under shear only, namely, the nominal mean shearing stress on a cross-section of a stud shank,

$\beta_x, \beta_y, \cdots, \beta_{xy}$: the stress concentration factors for each stress component under shear only.

Now, judging from the location of fatigue crack initiation, it would be natural to calculate the effective stress at the point Ap where the maximum stress concentration occurs. However, each stress component just at the point Ap or in a finite element including this point must be sensitively affected by the size of element meshes. Also, there may be a case that the point where the stress concentration occurs does not always coincide with the crack initiating point due to large variation in the shape of actual weld upset (e.g. height, diameter and angle, θ) or local defects at the toe of the upset. Therefore, it would be reasonable to pay attention to an average stress in some volume including the point Ap. The average value per unit volume for each stress component is calculated about four elements in the vicinity of the point Ap. As an example, the finite element analysis was conducted on a model for D-series specimen and the following equation was obtained:

$$\sigma_e=\sqrt{2.174\,\sigma_0^2+5.834\,\tau_0^2+6.521\,\sigma_0\cdot\tau_0} \qquad (3)$$

5.2 Evaluation of Test Results

The rearranged data by applying Eq.(3) to the test results for four different test series (C, D-1, D-2 and D-3) of the three kinds of steels (see Figs. 6 ∿ 8), are plotted in Fig.17 in terms of the effective stress range, σ_{er} . A S-N curve and a scatter band (σ means standard deviation) of all the points which were determined by using the least square method, are also shown in the figure. Most of the points are distributed in a comparatively narrow scatter band, though they vary somewhat widely at the cycle lives larger than one million cycles.
From the fact that all of the data formed a well-arranged S-N relationship irrespective of shear stress levels or steel grades, it was recognized that the fatigue strength of plates with welded studs under combined tension and shear could be reasonably evaluated by the effective stress.

Next, the beam-type test results in Table 1 are compared with the coupon-type ones for SS41 steel by using the effective stress as shown in Fig. 18. The S-N curve and scatter band were obtained for the coupon-type test data only. The beam test results scatter near the upper bound of the scatter band, being distributed nearly parallel to the S-N curve of the plate. The difference between them might be caused mainly by over-estimation of stud forces in the beam specimens, because the stiffeness of cracked concrete slab could not be exactly assumed in the

incomplete interaction analysis. Taking into consideration of such over-estimation of the stud forces, the fatigue characteristics in both beam-type and coupon-type tests could be consistently interpreted by means of the effective stress. Besides, it may be said that the fatigue strength of the flange on which the studs are welded can be estimated sufficiently by the coupon-type test data.

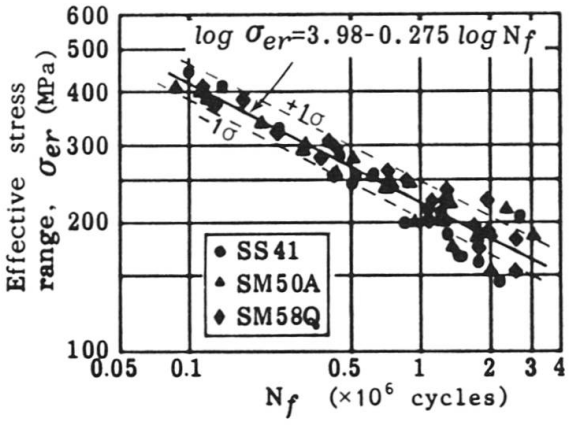

Fig. 17 S-N relations for effective stress.

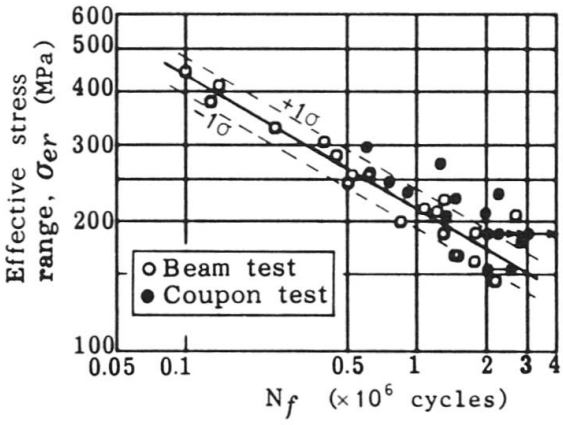

Fig. 18 Comparison of fatigue data between beam tests and coupon tests for SS41.

6. FATIGUE DESIGN PROPOSAL

When the fatigue assessment of the flange plate with stud shear connectors under a combined tension and shear loading is carried out in the design of structures, no applicable provision is found in any fatigue design codes. For example, in the ECCS Fatigue Recommendations [9], a plate with a stud under plate tension only is classified into Detail Category 80 and the fatigue of the plate is assessed on the normal stress in the plate regarding the stud as a welded attachment (non-load-carrying weld). Moreover, the stud shear connector under shear only is also classified into Detail Category 80 and its fatigue is assessed on the shear stress at the weld upset regarding the stud as a welded connection (load-carrying weld). The plate with studs under combined loadings, however, can not be found in any given Detail Category. Then, in order to incorporate the findings obtained by the present study into a design code, the authors have tried to propose a convenient method for the fatigue assessment of the present detail using, as an example, the Recommendations.

The fatigue assessment is expressed analytically as follows:

$$\frac{\Delta \sigma_R}{\gamma_m} \geqq \gamma_s \Delta \sigma_E \qquad (4)$$

where $\Delta \sigma_R$: the fatigue strength defined as the stress range in Fig.19 corresponding to a given number of stress cycles,

$\Delta \sigma_E$: the equivalent constant amplitude stress range which is calculated from the design stress spectrum,

γ_m, γ_s : partial safety factors to be applied to the fatigue strength and the fatigue loading, respectively.

Fig.19 indicates the ECCS-TC6 fatigue strength curves for normal stress ranges and these curves represent the mean experimental value minus two standard deviations for the details classified.

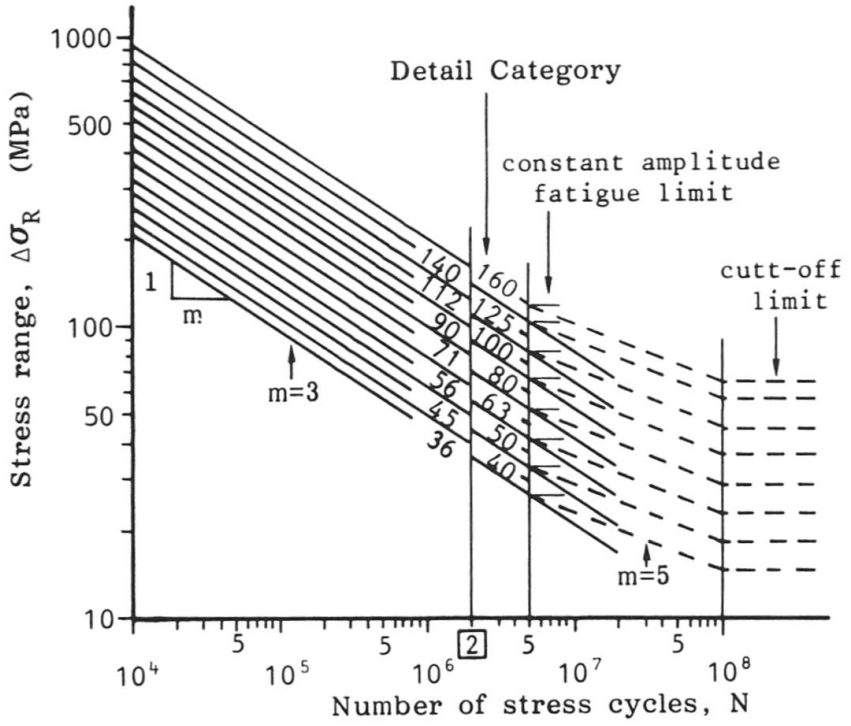

Fig. 19 ECCS-TC6 fatigue strength curves for normal stress ranges.

Since it was known from the present study that the fatigue strength of a plate with studs was reasonably evaluated by the effective stress, it can be proposed that $\Delta\sigma_R$ and $\Delta\sigma_E$ in Eq.(4) may be also estimated by using not the maximum principal stresses, but the effective stresses.
The lower confidence limit with minus two standard deviations for the present test data in Fig.17 can be expressed by a S-N curve with the slope constant of m =3.6 which nearly gives σ_{er} a value of 150 MPa at 2×10^6 cycles. The plate with studs under combined stress conditions might be conveniently classified into the Detail Category 140 on the safety side provided that a normal stress range on the ordinate in Fig.19 is regarded as an effective stress range. Then, the fatigue strength $\Delta\sigma_R$ could be determined in accordance with Chapter 6 (Fatigue Strength) in the Recommendations, although this classification results in a higher category in comparison with those for the above-mentioned similar cases due to the combined effects of normal and shear stresses on the fatigue strength.
Besides, the equivalent constant amplitude stress range, $\Delta\sigma_E$ are calculated on the effective stress at the base of the stud by using Eq.(3) with the nominal mean tensile stress on a cross-section of the plate, $\Delta\sigma_0$, and the nominal mean shearing stress on a cross-section of the stud shank, $\Delta\tau_0$, in accordance with Chapter 4 (Fatigue Loading) and Chapter 5 (Fatigue Stress Spectra). Partial safety factors γ_m and γ_s may be determined in accordance with Appendix C (Determination of the Safety Factors) in the Recommendations.
Thus, a convenient fatigue assessment of the flange plate with studs under a combined tension and shear loading could be conducted by evaluating $\Delta\sigma_R$ and $\Delta\sigma_E$ on the effective stresses.

7. CONCLUSIONS

As the results of the experimental and analytical studies on the fatigue characteristics of flange plates with welded studs in steel-concrete composite beams subjected to repeated negative moment, it may be concluded as follows:

(1) The fatigue strength of a steel plate with a stud under combined tension and shear decreases nearly in proportion to an increase in the shear force acting on the stud.

(2) In the plate with studs under any loading condition, the stress concentration occurs at the upset edge closest to the loading and the normal stress component in the loading direction predominates most.

(3) When the plate with studs is subjected to combined tension and shear at the same time, the state of 'overlapped stress concentration' occurs at the upset edge due to geometrical and dynamical discontinuity resulting in a very large stress concentration, of which magnitude can be approximately computed by the superposition of the stresses for each loading case.

(4) The effective stress in the vicinity of a crack initiation point is reasonable for the evaluation of the fatigue strength of the steel plate with studs, and its equation is as follows;

$$\sigma_e=\sqrt{2.174\,\sigma_0^2+5.834\,\tau_0^2+6.521\,\sigma_0\cdot\tau_0}$$

(5) According to S-N relations expressed in terms of the effective stress, the beam-type test results agree well with the coupon-type ones. The fatigue strength of the flange plates with welded studs can be estimated sufficiently by the coupon-type test data.

(6) Fatigue assessment of the flange plate with studs would be carried out by using effective stresses and applying Detail Category 140 in the ECCS Fatigue Recommendations.

REFERENCES

1. Selby, K.A., Stallmeyer, J.E. and W.H. Munse, Fatigue Tests of Plates and Beams with Stud Shear Connectors, Civil Engineering Studies, Structural Research Series No.270, University of Illinois, 1963.
2. Roshardt, W., Einfluss des Aufshweissens von Bolzen auf das Grundmaterial, Schweiz. Bauzeitung, 84, Heft 51, 1966.
3. Wakabayashi, T., Sawano, K. and M. Naruoka, Tensile Fatigue Tests of Steel Plates with a Stud, Bridge and Foundation Engineering, Vol.5, No.4, 1971. (in Japanese)
4. Kunihiro, T., Inoue, K. and M. Furushou, Bending Fatigue Tests of Rolled and Welded H-Beam with Studs, Civil Engineering Technical Notes, Vol.15, No.12, 1973. (in Japanese)
5. Welz, W. und G. Dennin, Dauerfestigkeit von Konstruktionen mit aufgeshweissten Bolzen, Schweissen und Schneiden, 33, Heft 2, 1981.
6. Kunihiro, T., Inoue, K. and M. Furushou, Bending Fatigue Tests of Rolled and Welded H-Beam, Civil Engineering Technical Notes, Vol.14, No.12, 1972. (in Japanese)
7. Maeda, Y. and Y. Kajikawa, Fatigue Behavior of Composite Beams Subjected to Negative Moment, Proc. of 16th National Symposium on Bridge and Structural Engineering, Tokyo, 1971.
8. Maeda, Y. and Y. Kajikawa, Fatigue Strength of Steel Plates with a Stud Shear Connector for Application to Continuous Composite Beams, Preliminary Report, 9th Congress of IABSE, 1972.
9. European Convention for Constructional Steelwork (ECCS), Recommendations for the Fatigue Design of Steel Structures, Oct., 1985.